Dalton
Transactions

An international journal of inorganic chemistry

This article can be cited before page numbers have been issued, to do this please use: O. Stetsiuk, V. Synytsia, S. R. Petrusenko, V. Kokozay, A. El-Ghayoury, J. Cano, F. Lloret, M. Julve, B. Fleury and N. Avarvari, *Dalton Trans.*, 2019, DOI: 10.1039/C9DT02503K.

ROYAL SOCIETY
OF CHEMISTRY

rsc.li/dalton

Co-existence of ferro- and antiferromagnetic interactions in a hexanuclear mixed-valence $Co^{III}_2Mn^{II}_2Mn^{IV}_2$ cluster sustained by a multidentate Schiff base ligand†

Oleh Stetsiuk,[ab] Valentyn Synytsia,[b] Svitlana R. Petrusenko,[b] Vladimir N. Kokozay,[b] Abdelkrim El-Ghayoury,[a] Joan Cano,*[c] Francesc Lloret,[c] Miguel Julve,[c] Benoit Fleury,[de] and Narcis Avarvari*[a]

Abstract

The successful utilization of the “direct synthesis” approach yielded the unprecedented hexanuclear complex of formula $[Co_2Mn^{II}_2Mn^{IV}_2(L^1)_4Cl_2(\mu_3\text{-}O)_2(dmf)_4]\cdot 2dmf$ (**1**) (H_3L is the Schiff base derived from the condensation of salicylaldehyde and 3-aminopropane-1,2-diol). Single crystal X-ray analysis revealed that **1** crystallizes in the monoclinic system $P2_1/c$ and it contains a rare mixed-valence $\{Co^{III}_2Mn^{II}_2Mn^{IV}_2(\mu_2\text{-}O)_8(\mu_3\text{-}O)_2\}$ core where all metal ions are linked through the phenolato and alkoxo groups of the L^{3-} ligand. Besides the charge balance resulting from the X-ray structure, the oxidation state of the metal ions has been confirmed by XPS spectroscopy. Cryomagnetic studies indicate the coexistence of ferro- (Mn^{IV}–Mn^{II}, $J_2 = +2.19(1)$ cm^{-1}, $J_3 = +1.10(1)$ cm^{-1}; Mn^{II}–Mn^{II}, $j = +0.283(3)$ cm^{-1}) and antiferromagnetic interactions (Mn^{IV}–Mn^{IV}, $J_1 = -17.31(4)$ cm^{-1}), the six-coordinate Co^{III} ions being diamagnetic. DFT type calculations were carried out to substantiate these values. The energy diagram for the different spin states using the best-fit parameters show the occurrence of six low-lying spin sates ($S = 0$-5) which are close in energy but clearly separated from the remaining ones, the ground spin stae being $S = 5$. Complex **1** is found to be the first example where weak ferromagnetic exchange between Mn^{II} ions through the long –O–Mn^{IV}–O– pathway takes place.

---

[a] *MOLTECH-Anjou, UMR 6200, CNRS, UNIV Angers, 2 bd Lavoisier, 49045 ANGERS Cedex (France). E-mail:* narcis.avarvari@univ-angers.fr

[b] *Department of Inorganic Chemistry, Taras Shevchenko National University of Kyiv, Volodymyrska str. 64/13, Kyiv 01601 (Ukraine).*

[c] *Instituto de Ciencia Molecular (ICMol)/Departament de Química Inorgànica, Universitat de València, C/Catedrático José Beltrán 2, 46980 Paterna (Valencia) (Spain). E-mail:* Joan.Cano@uv.es

[d] *Sorbonne Université, CNRS. Institut Parisien de Chimie Moléculaire, UMR 8232, F-75005 Paris (France)*

[e] *CNRS, UMR 8232, Institut Parisien de Chimie Moléculaire, F-75005 Paris (France)*

View Article Online
DOI: 10.1039/C9DT02503K

†Electronic supplementary information (ESI) available: Infrared spectrum (Fig. S1), XPS spectra (Figs. S2-S4), hydrogen bonding (Fig. S5), bond valence sum calculations (Table S1) and spin configuration of the manganese atoms (Table S2). CCDC reference number 1819913. For ESI and crystallographic data in CIF or other electronic format see DOI : 10.1039/xxxxx.

Introduction

High nuclearity heterometallic clusters are among the most promising investigation objects of modern coordination chemistry. On the one hand, the presence of several metals in one complex makes such compounds a perspective platform for developing materials possessing magnetic[1-2] and catalytic properties.[3-6] On the other hand, the abundance of 3d metals in nature can be a fertile field for modelling the active sites of enzymes. In this respect, the Mn/Co pair is among the most interesting combinations for developing polymetallic complexes. Thus, besides the opportunity to exist in several oxidation states and to form polynuclear architectures, heterometallic Mn/Co active sites are found in enzymes that catalyse vital processes such as nitrogen fixation and carbon dioxide reduction.[7-9] Recent series of Mn/Co cubane complexes described by Tilley and coll.[10-11] have been used as water oxidation catalysts (WOCs). Moreover, the quantitative addition of cobalt(II) acetate to the heterometallic cubane complex $[MnCo_3O_4(OAc)_5(py)_3]$ (HOAc = acetic acid and py = pyridine) afforded the pentametallic "dangler" compound of formula $[MnCo_4O_4(OAc)_6(NO_3)(py)_3]$,[12] which is reminiscent of the photosystem II's oxygen-evolving centre which generates dioxygen from water.[13] The oxygen-evolving complex (OEC) is a peculiar cofactor consisting of a $[Mn_3CaO_4]$ cubane core appended with a "dangling" Mn centre,[14-16] in which the manganese ions present variable oxidation states,[17] and for which several synthetic model systems have been reported.[18-20]

It is therefore of utmost importance to access polynuclear heterometallic mixed-valence manganese-based clusters as they can constitute valuable models for the manganese clusters occurring in the living systems, and to clearly demonstrate the co-existence of several manganese ions in different oxidation states along with the investigation of their magnetic properties. From structural and magnetic points of view, the Mn/Co heterometallic complexes show a large diversity ranging from simple binuclear antiferromagnetic complexes such as $[CoMn(L^{2,3})(AcO)]ClO_4{\cdot}dmf$, $[CoMn(L^{2,4})(AcO)]ClO_4$ ($L^{2,3}$ and $L^{2,4}$ are derived from the condensation of 2,6-diformyl-4-methylphenol, ethylenediamine, and 1,3-trimethylenediamine or 1,4-tetramethylenediamine),[21]

$[CoMnL(OAc)]ClO_4$ and $[CoMnL(NCS)]ClO_4$ (L is a macrocycle derived by the 2:1:1 condensation of 2,6-diformyl-4-methylphenol, ethylenediamine, and diethylenetriamine),[22] to polynuclear mixed-valence compounds $[Mn^{II}_2Mn^{III}Co^{III}_2(OH)(Htea)_3(H_2tea)(acac)_3](NO_3)_2\cdot 3CH_2Cl_2$ and $[Mn^{II}_2Mn^{III}_2Co^{III}_2(Htea)_4(OMe)_2(acac)_4](NO_3)_2\cdot 2MeOH$ (H_3tea = triethanolamine and Hacac = acetylacetone)[23] exhibiting intramolecular ferromagnetic exchange and single molecule magnet behaviour, respectively.

Most of the polynuclear complexes reported in literature so far have been obtained by applying the "serendipitous assembly" approach described by Winpenny.[24] A particular case of this approach consists of the "direct synthesis of complexes",[25] based on the use of zero-valent metals as reagents for the generation of heterometallic aggregates. Recent application of the "direct synthesis" strategy has been successful for the preparation of heterobimetallic Mn/Cu,[26] Cu/Fe,[27] Co/Fe,[28] mixed-valent Co/Cu[29] and as well as heterotrimetallic complexes,[30-31] possessing a diversity of sophisticated crystal structures and properties. Herein we report the direct synthesis of the heterometallic complex $[Co^{III}_2Mn^{II}_2Mn^{IV}_2(L^1)_4Cl_2(\mu_3\text{-}O)_2(dmf)_4]\cdot 2dmf$ (**1**), containing a very rare hexanuclear $\{Co^{III}_2Mn^{II}_2Mn^{IV}_2(\mu\text{-}O)_8(\mu_3\text{-}O)_2\}$ core with co-existence of Mn^{II} and Mn^{IV} centres, showing intriguing magnetic properties.

Results and discussion

Synthesis and infrared spectroscopy

The open air reaction of cobalt powder and manganese chloride tetrahydrate in the presence of the multidentate Schiff base ligand *N*-(propylene-2,3-diol)salicylideneimine (H_3L^1), derived from salicylaldehyde and 3-aminopropane-1,2-diol (Scheme 1), affords a heterometallic complex possessing an extremely rare heterometallic Mn/Co cluster with a dicubane-like core (see below). Its formation can be explained if one considers the following reaction scheme:

$$2Co + 4MnCl_2\cdot 4H_2O + 4H_3L^1 + 2.5O_2 + 6Et_3N + 6dmf \rightarrow$$
$$[Co^{III}_2Mn^{II}_2Mn^{IV}_2(L^1)_4Cl_2(\mu_3\text{-}O)_2(dmf)_4]\cdot 2dmf\ (\mathbf{1}) + 6Et_3N\cdot HCl + 19H_2O.$$

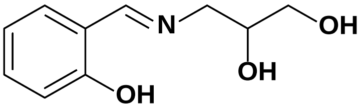

H_3L^1

Scheme 1. The polydentate Schiff base ligand H_3L^1.

The lack of O-H stretching vibrations in the high-frequency region of the infrared spectrum of **1** supports the presence of the fully deprotonated Schiff base $(L^1)^{3-}$ as ligand (Fig. S1, ESI). The occurrence of a strong absorption centred at ca. 1632 cm^{-1} is tentatively assigned to the ν(C=O) stretching vibration of dmf molecules[32] while the weak intense broad bands at 3100–2975 and 2975–2840 cm^{-1} attributed to ν(C–H) of the aromatic ring and aliphatic C–H bonds, respectively.

View Article Online
DOI: 10.1039/C9DT02503K

Crystal structure

Single crystal X-Ray analysis reveals that compound **1** crystallizes in the monoclinic system, space group $P2_1/c$ (Table 1) with half of the complex in the asymmetric unit (Fig. 1a). The structure of **1** is based on the heterometallic hexanuclear core $\{Co^{III}_2Mn^{II}_2Mn^{IV}_2(\mu\text{-}O)_8(\mu_3\text{-}O)_2\}$, where all the metal ions are linked through μ- and μ_3-O atoms from the deprotonated O-H groups of the Schiff base ligand (Fig. 1b). According to CSD, a hexanuclear core $\{M_6(\mu\text{-}X)_8(\mu_3\text{-}X)_2\}$, similar to that of **1**, was firstly described in 1993 for metal-antimony ethoxides of general formula $[M_2Sb_4(OEt)_{16}]$ (M = Mn, Mg, Ni),[33-34] and later on for 3d metals it has been described only for the homometallic Ni complex $(HNEt_3)_2[Ni_6(ntba)_4(\mu_3\text{-}OH)_2(\mu\text{-}OH_2)_2]\cdot 5CH_3CN\cdot 2.6H_2O$ (H_3ntba = 2,2′,2″-nitrilotribenzoic acid).[35] Recently, this core was also observed for a series of 3d-4f $Mn^{III}_4Ln^{III}_2$ (Ln = Sm, Gd and Dy) complexes with a Schiff base ligand derived from of *o*-vanillin and 3-aminopropane-1,2-diol.[36] Thereby, complex **1** is found to be the first example of heterometallic 3d metal complex possessing hexanuclear mixed-valence dicubane-like core with a rare co-existence of Mn^{II} and Mn^{IV} oxidation states.

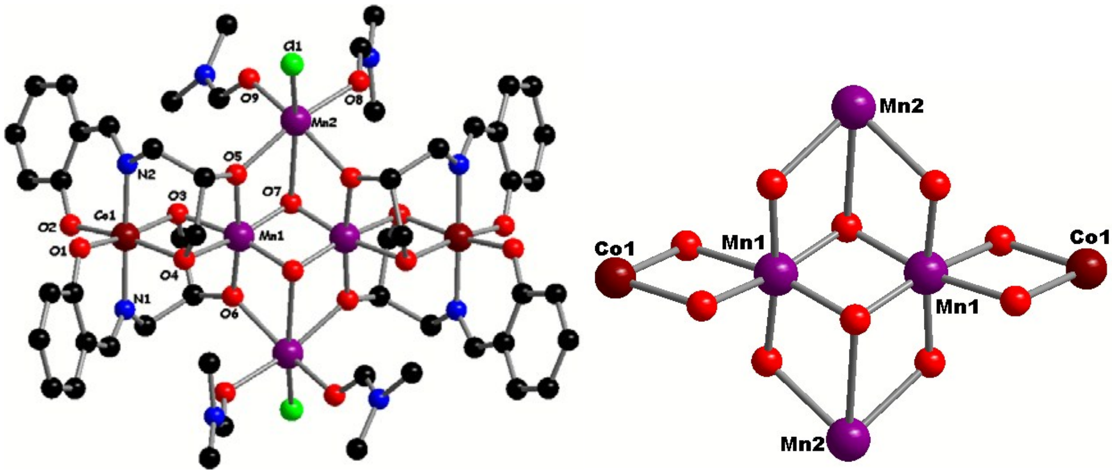

a b

Fig. 1 (a) View of the crystal structure of **1** with atom labelling (the hydrogen atoms and the crystallization dmf molecules were omitted for clarity). (b) Ball-and-stick representation of the $\{Co^{III}_2Mn^{II}_2Mn^{IV}_2(\mu\text{-}O)_8(\mu_3\text{-}O)_2\}$ molecular core.

Table 1 Summary of the crystal data and structure refinement for **1**

View Article Online
DOI: 10.1039/C9DT02503K

Formula	$C_{58}H_{82}Cl_2Co_2Mn_4N_{10}O_{20}$
M [g·mol^{-1}]	1647.86
Crystal system	monoclinic
Space group	$P2_1/c$
a [Å]	8.5730(2)
b [Å]	21.4804(4)
c [Å]	18.9257(4)
β [°]	91.632(2)
V [Å$^{3]}$	3483.78(13)
Z	2
P$_{calcd.}$ [g/cm$^{3]}$	1.571
μ [mm^{-1}]	10.722
F(000)	1696
Goodness-of-fit on F^2	1.042
T [K]	150
2Θ$_{max}$	140
R_{int}	0.0214
final R_1/wR_2 [$I > 2\sigma(I)$]	0.0284/ 0.0337
R_1/wR_2 (all data)	0.0738/ 0.0771
Largest difference peak/hole (e·Å^3)	0.646/-0.391

Table 2 Selected geometrical parameters (distances/Å and angles/°) for **1***

Mn1—O3	1.9825(14)	N1—Co1	1.9461(17)
Mn1—O4	1.9580(13)	N2—Co1	1.9455(16)
Mn1—O5	1.9117(13)	O1—Co1	1.8760(15)
Mn1—O6	1.9051(13)	O2—Co1	1.8858(14)
Mn1—O7	1.8442(13)	O3—Co1	1.9389(14)
Mn1—O7^{i}	1.8379(14)	O4—Co1	1.9263(13)
Mn2—O5	2.1358(13)		
Mn2—O6^{i}	2.1007(14)		
Mn2—O8	2.1505(17)		
Mn2—O9	2.1645(15)		
Mn2—Cl1	2.4079(6)		
O7^{i}—Mn1—O7	85.21(6)	O1—Co1—O2	93.80(7)
O7^{i}—Mn1—O6	97.30(6)	O1—Co1—O4	91.14(6)
O7—Mn1—O6	87.17(6)	O2—Co1—O4	169.57(6)
O7^{i}—Mn1—O5	86.33(6)	O1—Co1—O3	168.53(6)
O7—Mn1—O5	99.37(6)	O2—Co1—O3	92.27(6)
O6—Mn1—O5	172.80(6)	O4—Co1—O3	84.49(6)
O7^{i}—Mn1—O4	168.46(6)	O1—Co1—N2	86.42(7)
O7—Mn1—O4	95.53(6)	O2—Co1—N2	93.73(7)
O6—Mn1—O4	94.24(6)	O4—Co1—N2	95.74(6)
O5—Mn1—O4	82.18(6)	O3—Co1—N2	83.48(6)
O7^{i}—Mn1—O3	99.03(6)	O1—Co1—N1	94.21(7)
O7—Mn1—O3	168.24(6)	O2—Co1—N1	87.29(7)
O6—Mn1—O3	81.43(6)	O4—Co1—N1	83.19(6)
O5—Mn1—O3	91.88(6)	O3—Co1—N1	95.79(6)
O4—Mn1—O3	82.52(6)	N2—Co1—N1	178.77(7)

View Article Online
DOI: 10.1039/C9DT02503K

O6^i—Mn2—O5	87.89(5)
O6^i—Mn2—O8	86.64(6)
O5—Mn2—O8	164.70(7)
O6^i—Mn2—O9	152.50(6)
O5—Mn2—O9	96.17(6)
O8—Mn2—O9	82.37(6)
O6^i—Mn2—Cl1	103.39(4)
O5—Mn2—Cl1	97.68(4)
O8—Mn2—Cl1	97.48(6)
O9—Mn2—Cl1	103.00(4)

*Symmetry code: (i) = 1–*x*, 1–*y*, 1–*z*.

Each cobalt(II) ion in **1** has a distorted octahedral surrounding CoN_2O_4 which is formed by the donor atoms of two Schiff bases (CoN_2O_4 unit). The NOO donor set of each Schiff base exhibits a *fac*-arrangement with the two nitrogen atoms in a *trans* disposition. The values of the Co-(O)N bond lengths are in the range 1.8775(14)–1.9478(16) Å and those of the *cis*-/*trans*-angles are 83.505(60)–95.736(62)˚ and 168.547(59)–178.742(67)˚, respectively (Table 2). Analysis of the bond lengths with further bond valence sum (BVS)[37-39] calculation for Co (Table S1) ion allows us to consider its oxidation state as +3, a conclusion which is in agreement with other examples of cobalt-containing complexes described in literature.[40] The above-mentioned oxidation state was also confirmed by X-ray photoelectron spectroscopy (XPS), a technique that has been widely used for the determination of the elements and the oxidation states of metal ions thanks to spin-multiplet splitting features of their core level peaks. Multiplet splitting of a photoelectron peak occurs when the photoelectron interacts with unpaired valence electrons and is observed for Mn 3s and Co $2p_{3/2}$ levels.[41] The Co2p XPS spectrum displays the characteristic spin-orbit $2p_{3/2}$ and $2p_{1/2}$ peaks split by 15 eV at 780.5 eV and 795.5 eV respectively (Fig. S2), a value in accordance with trivalent Co ions.[42-44] More convincing, the $2p_{3/2}$ level does not show any spin-multiplet satellite, proving the diamagnetic trivalent oxidation state for the cobalt centres.

The oxidation states of both types of Mn ions (Mn1 and Mn2) were established to be +II (Mn2) and +IV (Mn1), which was further confirmed by the BVS calculation (Table S1), magnetic and XPS measurements. Regarding the determination of the average oxidation state (AOS) by XPS, the closest analogy of this complex can be made with the tetranuclear $Mn^{II}_2Mn^{IV}_2$ mixed-valence clusters, described by Tong *et al.*[45] where the oxidation states have been proved by considering the Mn2p XPS spectrum. Indeed, analysis of the Mn2p XPS data for complex **1** gives the values 641.8 and 635.4 eV of the binding energies (Fig. S3), which are indicative of the presence of Mn^{IV} ions. Considering spin multiplet splitting of the Mn3s edge, examples of XPS spectra of molecular compounds are scarce and the best analogy we could find is the one with the $[Mn_{12}O_{12}(O_2CCH_2C(CH_3)_3)_8(O_2CCHCl_2)_8(H_2O)_4]$ (Mn_{12}) complex in which the AOS is +3.3 and for which the Mn3s splitting is 5.50 eV.[46] The Mn3s XPS spectrum of **1** (Fig. S4) reveals a spin multiplet with an energy splitting of 5.57 eV. The slightly higher value of this splitting for **1** in comparison to the one of Mn_{12} is in good agreement with the slightly lower AOS of +3 in complex **1**; indeed, the lower the AOS, the larger the splitting.

The coordination environment of the manganese ions of **1** is formed by oxygen (Mn1) and oxygen and chlorine (Mn2) donor atoms, resulting in distorted $Mn1O_6$ and $Mn2O_5Cl$ octahedral surroundings. The Mn1–O bond lengths are in the range 1.8380(14)–1.9823(14) Å, values which are shorter than those at Mn2 [2.1006(14)–2.5533(13) Å] as expected due to the lower oxidation state of this last metal atom. The remaining Mn2–Cl bond distance is equal to 2.4079(6) Å. It should be noted that the absence of Jahn-Teller distortion, which is typical for Mn^{III}-containing mixed-valence complexes,[47-51] may be also the aside statement of the oxidation state +IV for the Mn1 ions.

The values of the intermetallic metal-metal distances within the heterometallic core are 2.9115(6) (Co1···Mn1), 2.7103(6) (Mn1···Mn1) and 3.2936(5) Å (Mn1···Mn2). In the crystal packing numerous intermolecular van der Waals interactions between coordinated and uncoordinated DMF molecules and chloride anions were found [C–H···Cl: d(C27···Cl1) = 3,75 Å, ∠(C27–H27–Cl1) = 167°; d(C22···Cl1) = 3,66 Å, ∠(C22–H22C–Cl1) = 152°; d(C26···Cl1) = 3,64 Å, ∠(C26–H26B–Cl1) = 158°]. This allows us to consider complex **1** as a supramolecular 1D coordination polymer (Fig. S5).

The peculiarity of the crystal structure of **1** induced us to try to understand the possible ways for its formation. The analysis of some of the previous reports where the self-assembly of polynuclear compounds was described,[28,52,53] prompted us to propose a rational pathway for its formation (see Fig. 2).

View Article Online
DOI: 10.1039/C9DT02503K

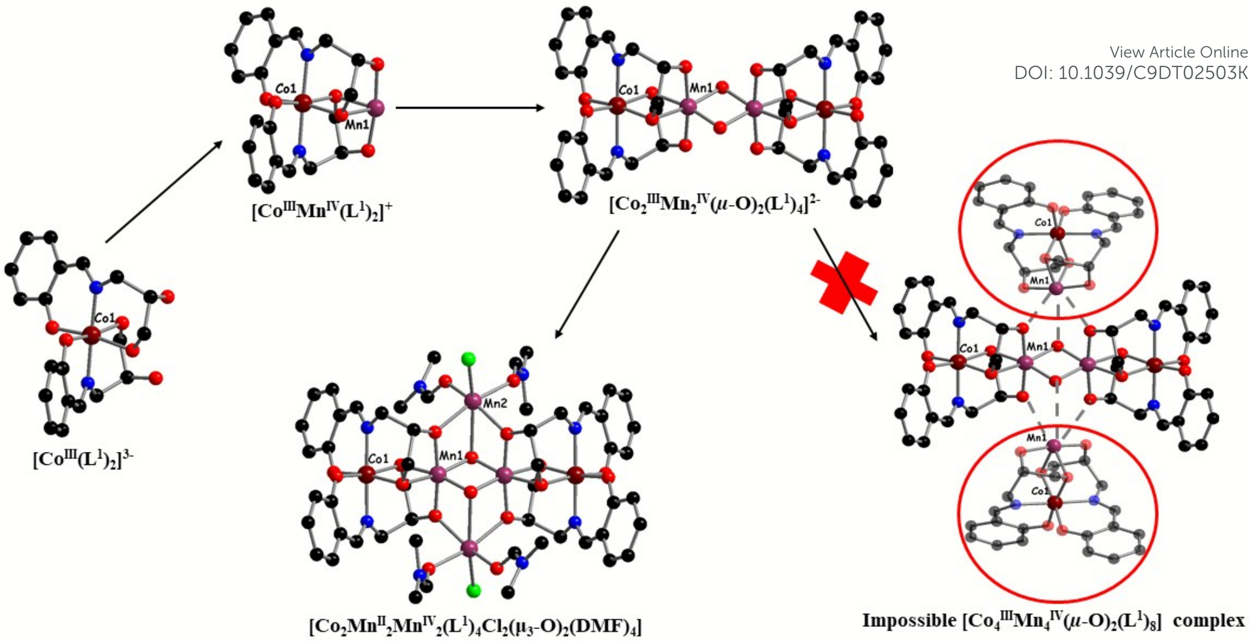

Fig. 2 Proposed pathway for the formation of **1**.

At the beginning, the coordination of the deprotonated Schiff base in the open air would lead to the formation of the $[Co^{III}(L^1)_2]^{3-}$ unit, possessing a typical N_2O_4 coordination environment for cobalt(III). The subsequent coordination of this unit to manganese ions through the alkoxo-groups of the ligand would allow the formation of the heterometallic $[Co^{III}Mn^{IV}(L^1)_2]^+$ species. The self-assembly of these two blocks would lead to the tetranuclear $[Co_2^{III}Mn_2^{IV(}\mu\text{-}O)_2(L^1)_4]^{2-}$ fragment. The presence of the oxo groups can be explained by the formation of water molecules during the Schiff base condensation. Then there are two possible routes of further self-assembly. The first one is the interaction of $[Co_2^{III}Mn_2^{IV}(\mu\text{-}O)_2(L^1)_4]^{2-}$, possessing the vacant coordination positions of unsaturated oxygen atoms, with the $[Co^{III}Mn^{IV}(L^1)_2]^+$ species. As a result of such assembly process, the octanuclear $[Co_4^{III}Mn_4^{IV}(\mu\text{-}O)_2(L^1)_8]$ complex would have been obtained. Most likely, the steric hindrance of the bulky benzene rings prevents the formation of the octanuclear complex. Moreover, an excess of Mn^{II} ions in the reaction mixture, which are solvated by the dmf molecules, forces the interaction of the $[Co_2^{III}Mn_2^{IV}(\mu\text{-}O)_2(L^1)_4]^{2-}$ fragment with the less bulky $[MnCl(dmf)_x]^{2+}$ units to yield **1**.

Magnetic properties and DFT type calculations

The magnetic properties of **1** in the form of $\chi_M T$ against T plot [χ_M is the magnetic susceptibility per $Co^{III}_2Mn^{II}_2Mn^{IV}_2$ unit] are shown in Fig. 3. At room temperature, $\chi_M T$ is equal to 12.45 cm^3 mol^{-1} K, a value which is as expected for a set of two manganese(II) and two manganese(IV) ions magnetically isolated, ($\chi_M T = 2\ (4.375 + 1.875) = 12.5$ cm^3 mol^{-1} K with $S_{Mn(II)} = 5/2$, $S_{Mn(IV)} = 3/2$ and $g_{Mn(II)} = g_{Mn(IV)} = 2.0$), the cobalt(III) ions being diamagnetic. Upon cooling, $\chi_M T$ steadily

View Article Online
DOI: 10.1039/C9DT02503K

decreases to reach a minimum of 10.27 cm^3 mol^{-1} K at 5.0 K and it further increases to 11.20 cm^3 mol^{-1} K at 1.9 K. The shape of this curve in the high temperature domain indicates the occurrence of a dominant antiferromagnetic interaction between some of the paramagnetic centres. The increase of $\chi_{\mathrm{M}}T$ after the minimum at low temperatures could be the result of the co-existence of ferro- and antiferromagnetic interactions (see below) and/or to the non-compensation of the average Landé factors of the interacting manganese cations. This last assumption has to be discarded because of the practically identical values of the *g* factors of Mn(II) and Mn(IV) cations. Neither in-phase nor out-of-phase signals were observed for **1** under zero or non-zero applied dc magnetic fields down to 1.9 K.

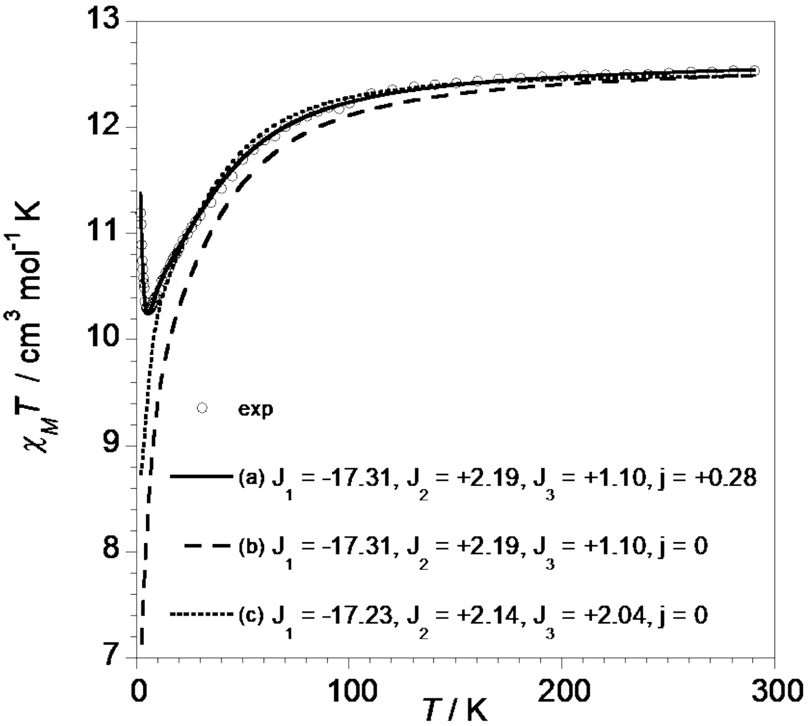

Fig. 3 Temperature dependence of $\chi_{\mathrm{M}}T$: (o) experimental; (—), (−−) and (···) best-fit curves through eq (1) (see text).

An inspection of the crystal structure of **1**, reveals the presence of several intramolecular exchange pathways: (i) the double oxo bridge for Mn1/Mn1$^{\mathrm{i}}$ (J_1); (ii) the alkoxo and oxo bridges for Mn1/Mn2 (and Mn1$^{\mathrm{i}}$/Mn2$^{\mathrm{i}}$) (J_2) and Mn1/Mn2$^{\mathrm{i}}$ (and Mn1$^{\mathrm{i}}$/Mn2) (J_3); and (iii) the multiatom second-neighbour for Mn2/Mn2$^{\mathrm{i}}$ (*j*) (see Scheme 2). Consequently, the appropriate spin Hamiltonian to analyse the magnetic data of **1** would be given by eq (1):

$$\hat{H} = -J_1\hat{S}_1\hat{S}_{1\mathrm{i}} - J_2\left(\hat{S}_1\hat{S}_2 + \hat{S}_{1\mathrm{i}}\hat{S}_{2\mathrm{i}}\right) - J_3\left(\hat{S}_1\hat{S}_{2\mathrm{i}} + \hat{S}_{1\mathrm{i}}\hat{S}_2\right) - j\hat{S}_2\hat{S}_{2\mathrm{i}} + g\beta H(\hat{S}_1 + \hat{S}_{1\mathrm{i}} + \hat{S}_2 + \hat{S}_{2\mathrm{i}})$$

where g is the average Landé factor which is assumed to be identical for the manganese(II) and manganese(IV) ions.

View Article Online
DOI: 10.1039/C9DT02503K

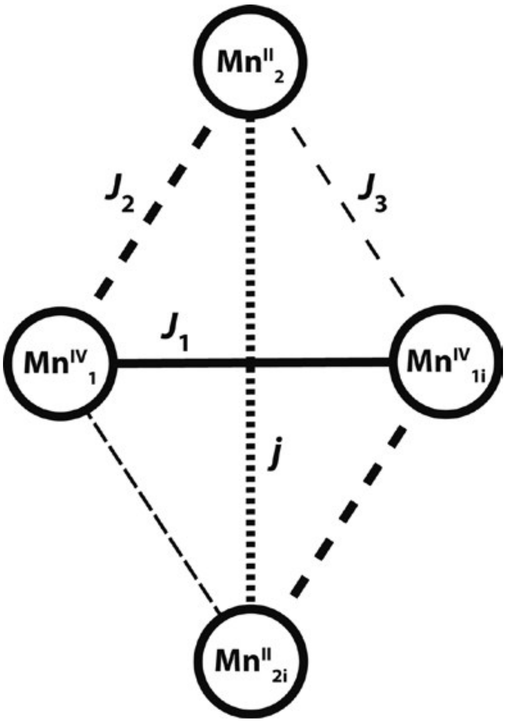

Scheme 2. Exchange coupling pattern in **1**.

Nevertheless, prior to perform this analysis, and having in mind the uncommon tetranuclear mixed-valence $Mn^{II}_2Mn^{IV}_2$ motif in **1** where each oxo bridge connects one Mn(II) (Mn2 or Mn2^{i}) with two Mn(IV) (Mn1 or Mn1^{i}) ions,[45, 54-56] we have considered another structural alternative: a $Mn^{III}_2Mn^{II}_2$ cluster where the two oxo bridges would be hydroxo groups and each Mn(IV) becomes Mn(III). DFT type calculations on the two structural possibilities were carried out. Focusing first on the $Mn^{II}_2Mn^{IV}_2$ model, the results displayed in Table 3 indicate the co-existence of the ferro- and antiferromagnetic couplings. The fact that the antiferromagnetic interaction is the dominant one accounts for the shape of the $\chi_M T$ plot in the high temperature domain. However, the standard deviations of the $J_{1\text{-}3}$ parameters are relatively high, a feature that can be due to the presence of the 2nd neighbour interactions. The inclusion of the j coupling causes a significant decrease of these deviations and, even though they are larger than usual (most likely because of a partial charge transfer between the Mn^{IV} ions and the oxo bridges), they can be considered correct. This additional magnetic coupling (j) is weak (as expected) and ferromagnetic. Dealing with the second model ($Mn^{III}_2Mn^{II}_2$), the standard deviation for the magnetic coupling constants, independently on the incorporation of the j parameter, are uncommonly large, even greater than the calculated J_i values. Therefore, this model should be ruled out.

Once the possibility of the $Mn^{III}_2Mn^{II}_2$ model is discarded, the treatment of the magnetic data of the $Mn^{IV}_2Mn^{II}_2$ motif through eq (1) by the *VPMAG* program[57] was carried out considering first $j = 0$ and fixing $g = 2.0$. The best-fit parameters are $J_1 = –17.23(4)$ cm^{-1}, $J_2 = +2.14(1)$ cm^{-1}, $J_3 = +2.04(1)$ cm^{-1} (set a). This model (dotted line in Fig. 3) matches well the magnetic data until 10

View Article Online
DOI: 10.1039/C9DT02503K

K, but it is unable to reproduce the minimum and the further increase of $\chi_M T$ at very low temperatures. The second approach incorporating j as variable parameter reproduces very well the magnetic data in the whole temperature range explored (solid line in Fig. 3), the best-fit parameters being $J_1 = -17.31(4)$ cm^{-1}, $J_2 = +2.19(1)$ cm^{-1}, $J_3 = +1.10(1)$ cm^{-1}, and $j = +0.283(3)$ cm^{-1} (set b). These results together with those from theoretical calculations give support to the reliability of the occurrence of the weak 2nd neighbour magnetic interaction between Mn^{II} ions. Finally, in order to illustrate the influence of the j parameter on the shape of the $\chi_M T$ plot, we performed the last simulation of the magnetic data with $J_1 = -17.31(4)$ cm^{-1}, $J_2 = +2.19(1)$ cm^{-1}, $J_3 = +1.10(1)$ cm^{-1}, and fixing $j = 0$ cm^{-1} (set c). The calculated $\chi_M T$ plot (dashed line in Fig. 3) follows the shape of the magnetic data in the high temperature domain being always below them, and it sharply decreases at low temperatures, being unable to reproduce the minimum and the further increase of $\chi_M T$ below 10 K. This feature reveals the determinant character of the weak ferromagnetic coupling j to simulate the magnetic data of **1**.

In order to illustrate the influence of the spin coupling pattern on the energy of the different spin states, and indirectly on the magnetic behaviour, the energy diagram for the different spin states using the best-fit parameters from set (b) is shown in Fig. 4a. One can see in this picture that six low-lying spin states (S = 0–5) are clearly separated from the remaining ones, the ground spin state being S = 5. These low-lying states are very close in energy as shown the magnification shown in Fig. 4b. This fact reveals that small variations of certain magnetic couplings can modify the nature of the ground spin state. Fig. 5 is very illustrative in this respect. In such a case, any of the six low-lying spin states could be the ground state through a small variation of j in the range of 0.06 to 0.14 cm^{-1}.

Table 3 Selected magneto-structural data for **1**

Magnetic Coupling	Bridges	Centres	$d_{\mathrm{Mn-Mn}}$ (Å)	$\mathrm{Mn}\widehat{\mathrm{O}}\mathrm{Mn}$ (deg)	J_{calc} (cm^{-1})	J_{exp} (cm^{-1})
J_1	μ_3-O μ_3-O	$\mathrm{Mn}_1^{\mathrm{IV}} - \mathrm{Mn}_{1^{\mathrm{i}}}^{\mathrm{IV}}$	2.710	94.37 94.87	−19.2(4)	−17.31(4)
J_2	μ-OR μ_3-O	$\mathrm{Mn}_1^{\mathrm{IV}} - \mathrm{Mn}_2^{\mathrm{II}}/\mathrm{Mn}_{1^{\mathrm{i}}}^{\mathrm{IV}} - \mathrm{Mn}_{2^{\mathrm{i}}}^{\mathrm{II}}$	3.329	110.57 97.52	+4.07(13)	+1.10(1)
J_3	μ-OR μ_3-O	$\mathrm{Mn}_{1^{\mathrm{i}}}^{\mathrm{IV}} - \mathrm{Mn}_2^{\mathrm{II}}/\mathrm{Mn}_1^{\mathrm{IV}} - \mathrm{Mn}_{2^{\mathrm{i}}}^{\mathrm{II}}$	3.294	110.52 95.86	+6.93(13)	+2.10(1)
j	μ-(OMn$^{\mathrm{IV}}$O) μ-(OMn$^{\mathrm{IV}}$O)	$\mathrm{Mn}_2^{\mathrm{II}} - \mathrm{Mn}_{2^{\mathrm{i}}}^{\mathrm{II}}$	6.043	-----	+0.29(15)	+0.283(3)

View Article Online
DOI: 10.1039/C9DT02503K

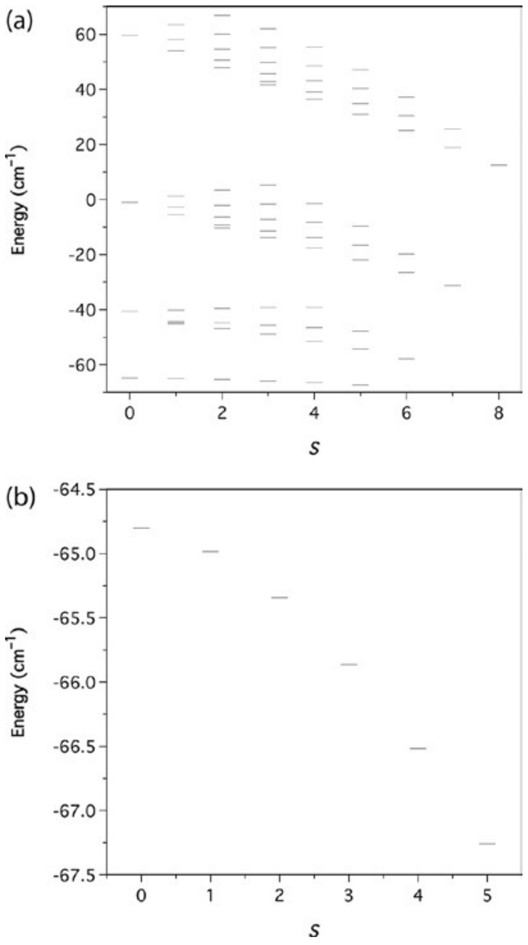

Fig. 4 (Top) Energy levels for the spin states of **1** by using the isotropic exchange parameters of the set (b). (Bottom) A detail of the energy levels of the low-lying S = 0–5 spin states for **1**.

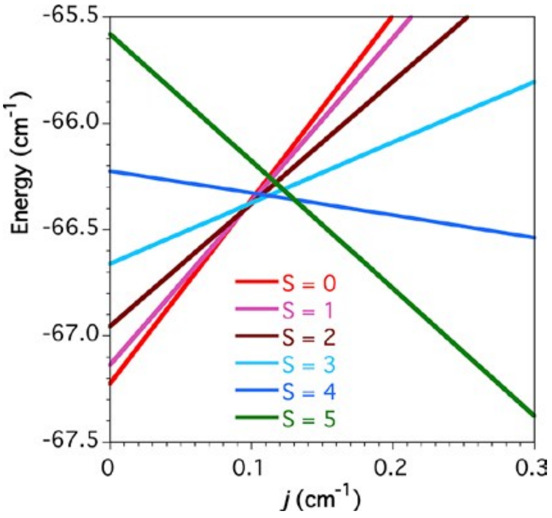

Fig. 5 Energy of the low-lying S = 0–5 spin states of **1** as a function of the j parameter. Data obtained through the values of J_1, J_2 and J_3 of the set (b).

Let us to finish this interpretation by discussing the nature and magnitude of the magnetic couplings in **1**. The antiferromagnetic coupling between the Mn(IV) ions through the double-oxo bridges (J_1) is comparable to the value obtained for this coupling in the $[Mn^{II}_2Mn^{IV}_2O_2(heed)_2(EtOH)_6Br_2]Br_2$ [H_2heed = *N*,*N*-bis(2-hydroxyethyl)ethylene diamine] (J = –23.8 cm^{-1}),[56] where with this type of exchange pathway occurs. In such a case, the values of the angle at the bridgehead oxo atom [Mn-O-Mn = 96.18(8)°] and the intramolecular $Mn^{IV}\cdots Mn^{IV}$ distance (96.2° and 2.71 Å) are comparable to those in **1** (94.6° and 2.71 Å). However, there are also examples with stronger magnetic couplings (–J values in the range 96–164 cm^{-1}) for similar systems but having shorter intramolecular intermetallic distances.[58] In this respect, theoretical calculations demonstrated that this kind of magnetic coupling is very sensitive to the value of the intermetallic $Mn^{IV}\cdots Mn^{IV}$ metal distance and, consequently, to the Mn–O_{oxo}–Mn angle. Moreover, other factors as geometrical distortions of the coordination sphere or the electronic nature of the peripheral ligands can play a significant role. Anyway, the relatively strong antiferromagnetic coupling found for J_1 in **1** is within normal expectations. As far as the Mn^{IV}–Mn^{II} couple in **1** is concerned, a μ_3-oxo and one alkoxo atoms act as bridges between these two cations. Given that magneto-structural studies on the Mn^{IV}–Mn^{II} pair are very scarce[45,54-56] the unambiguous determination of the magnetic coupling between these ions remains an open question. The closer example in the literature to this fragment in **1** is represented by the compound of formula $[Mn^{II}_2Mn^{IV}_2(\mu_4\text{-Hedte})_2(thme)_2]\cdot 2MeOH$ [H_4edte = *N*,*N*,*N'*,*N'*-tetrakis(2-hydroxyethyl)ethylenediamine and H_3thme = 1,1,1-tris(hydroxymethyl)ethane] where a double alkoxo group acts as bridge.[45] The magnetic coupling through this pathway in such a compound is J = +2.91 cm^{-1}, a value which is of the same nature and comparable size to those found in **1** for the Mn^{IV}–Mn^{II} pair (J_2 = +1.10 cm^{-1} and J_3 = +2.10 cm^{-1}). The electronic configurations of the six-coordinate Mn^{IV} and Mn^{II} ions are $t_{2g}^3e_g^0$ and $t_{2g}^3e_g^2$ respectively. Then, the contributions involving the t_{2g} magnetic orbitals of both metal ions are mostly antiferromagnetic and those entailing the t_{2g} from Mn^{IV} and e_g from Mn^{II} are ferromagnetic because of the strict orthogonality between the interacting magnetic orbitals. The larger spin delocalization of the e_g against t_{2g} orbitals provokes that the last contributions are dominant and a weak ferromagnetic net coupling for J_2 and J_3 is expected. Finally, as far as we are aware, no examples are reported dealing with magnetic interactions between Mn^{II} ions through the long –O–-Mn^{IV}–O– pathway (j). However, a very weak magnetic coupling is what one could predict for this pathway given the multiatom set involved, but a clear-cut answer to the origin of its ferromagnetic nature is precluded.

Conclusions

The open air reaction of cobalt powder, manganese(II) chloride in a DMF solution containing the polydentate Schiff base ligand H_3L^1 allowed us to obtain the unprecedented hexanuclear Co/Mn complex **1**. It is the first example of heterometallic 3d-metal complexes possessing the mixed-valence core $\{Co^{III}_2Mn^{II}_2Mn^{IV}_2(\mu\text{-}O)_8(\mu_3\text{-}O)_2\}$ with a rare co-existence of Mn^{II} and Mn^{IV} centres. The presence of several metal ions in different oxidation states has a paramount importance in many chemistry areas ranging from bioinorganic, as possible models for metalla-enzymes such as the oxygen evolving centre (OEC), to molecular magnetism in the search for tunable spin state complexes. The proposed pathway of the formation of **1** may be a small piece of the jigsaw of the self-assembly approach towards heterometallic compounds. The cryomagnetic study of **1** shows the co-existence of ferro- and antiferromagnetic interactions and reveal that the complex herein is the first example where magnetic interactions between Mn^{II} ions can be mediated through the long -O-Mn^{IV}-O- bridge.

Experimental section

General procedures

Reactions were carried out under air using HPLC solvents. IR spectra were recorded on ATR Bruker Vertex 70 spectrophotometer in the 4000−400 cm^{-1} range. Elemental analyses were recorded using a Flash 2000 Fisher Scientific Thermo Electron analyzer and the metals determination was performed by atomic absorption spectroscopy at the Department of Chemistry, Taras Shevchenko National University of Kyiv.

Synthesis of $[Co^{III}_2Mn^{II}_2Mn^{IV}_2(L^1)_4Cl_2(\mu_3\text{-}O)_2(dmf)_4]\cdot 2dmf$ (1). Salicylaldehyde (0.1 mL, 1.0 mmol), 3-aminopropane-1,2-diol (0.09 g, 1.0 mmol) and triethylamine (0.28 mL, 2.0 mmol) were dissolved in DMF (20 mL), forming a yellow solution of H_3L^1 which was stirred at 100–120 °C during 10-15 min. Then, cobalt powder (0.06 g, 1.0 mmol) and manganese(II) chloride tetrahydrate (0.2 g, 1.0 mmol) were added to the hot yellow solution of the ligand and stirred until the total dissolution of the cobalt(II) powder was observed (2 h). Dark brown crystals of **1** suitable for X-ray analysis were obtained from the reaction mixture upon diffusion of diethyl ether after few days. Yield: 0.25 g in pure crystalline state, 15% (per Mn). Anal. calc. for $C_{58}H_{82}Cl_2Co_2Mn_4N_{10}O_{20}$: C, 42.27; H, 5.02; N, 8.50; Mn, 13.34; Co, 7.15. Found: C, 42.05; H, 5.00; N, 8.40; Mn, 13.25; Co, 7.06%. IR (KBr, cm^{-1}): 2930 (w), 2870 (w), 1635 (s), 1533 (s), 1445 (s), 1399 (m), 1290 (s), 1190 (m), 1140 (s), 1040 (s), 935 (m), 900 (m), 755 (s), 656 (s), 590 (m), 530 (w), 467 (m), 435 (m). Compound **1** is soluble in dmso and dmf, sparingly soluble in MeOH and MeCN and insoluble in water.

Physical measurements

Variable-temperature (1.9-290 K) direct current (dc) magnetic susceptibility measurements under applied dc fields of 0.5 T ($T \geq 50$ K) and 250 G ($T < 50$ K) and variable field (0-5 T) were carried out on crushed crystals of **1** with a Quantum Design SQUID magnetometer. Alternating current (ac) magnetic susceptibility measurements in the temperature range 2.0 -12 K) under different applied static fields in the range 0–2.5 kG were performed on a Quantum Design Physical Property Measurement System (PPMS). The experimental magnetic susceptibility an magnetization data were corrected for the diamagnetic contributions of the constituent atoms and the sample holder (a plastic bag).

Computational details

DFT calculations were carried out through the Gaussian 09 package to estimate the magnitude of the magnetic coupling between the magnetic centres in **1**.[59] These calculations were performed with the B3LYP hybrid functional, the quadratic convergence approach and a guess function generated with the fragment tool from the same program.[60-62] Triple-ζ and double-ζ all-electron basis sets proposed by Ahlrichs *et al.* were employed for the metal atoms and the rest, respectively.[63,64] The magnetic coupling states were obtained from the relative energies of the broken-symmetry (BS) singlet spin states from the high-spin state with parallel local spin moments (see Table S2). More details about the use of the broken-symmetry approach to evaluate the magnetic coupling constants can be found in the literature.[65-67] A polarizable continuum model (PCM) was introduced in the calculations with the parameters corresponding to the acetonitrile.[68]

X-ray crystallography

Single crystal X-ray diffraction data were collected on an Agilent Technologies SuperNova diffractometer equipped with AtlasCCD detector and micro-focus Cu-Kα radiation (λ = 1.54184 Å). The structures were solved by direct methods and refined on F^2 by full matrix least-squares techniques using SHELX97 package.[69] All non-hydrogen atoms were refined anisotropically and multiscan empirical absorption was applied using CrysAlisPro program.[70] The hydrogen atoms were included in the geometrically calculated position and refined riding on the corresponding atom. Crystallographic data andrefinement statistics are given in Table 1 whereas main bond lengths and angles are listed in Table 2. The crystallographic drawings were performed by means of the Diamond program.[71] CCDC 1819913 contains the supplementary crystallographic data for this paper. This data can be obtained free of charge from The Cambridge Crystallographic Data Centre via www.ccdc.cam.ac.uk/data_request/cif.

View Article Online
DOI: 10.1039/C9DT02503K

ORCID

Vladimir Kokozay: 0000-0003-1834-3020
Joan Cano: 0000-0002-7382-7135
Francesc Lloret: 0000-0003-2959-0879
Miguel Julve: 0000-0001-9006-8268
Narcis Avarvari: 0000-0001-9970-4494

Conflicts of interest

There are no conflicts of interest to declare.

Acknowledgements

This work was supported in France by the CNRS, the University of Angers, in Ukraine by the Ministry of Education and Science, the Taras Shevchenko National University of Kyiv and the French Embassy in Kyiv (grant to O.S.), and in Spain by the Ministerio Español de Economía y Competitividad (Projects CTQ2016-75068P and CTQ2016-75671P) and the Unidad de Excelencia María de Maetzu (Project MDM2015-0538). Marion Giraud (University of Paris Diderot) is gratefully acknowledged for her assistance with the XPS measurements.

References

1 M. Andruh, J.-P. Costes, C. Diaz and S. Gao, *Inorg. Chem.* 2009**, 48**, 3342-3359.

2 Y.-Z. Zheng, G.-J. Zhou, Z. Zheng and R. E. P. Winpenny, *Chem. Soc. Rev.* 2014**, 43**, 1462-1475.

3 W.-X. Gao, H.-N. Zhang and G.-X. Jin, *Coord. Chem. Rev.* 2019**, 386**, 69-84.

4 D. S. Nesterov and O. V. Nesterova, *Catalysts* 2018**, 8**, 602.

5 D. S. Nesterov, O. V. Nesterova and A. J. L. Pombeiro, *Coord. Chem. Rev.* 2018**, 355**, 199-222.

6 O. V. Nesterova, K. V. Kasyanova, E. A. Buvaylo, O. Y. Vassilyeva, B. W. Skelton, D. S. Nesterov and A. J. L. Pombeiro, *Catalysts* 2019**, 9**, 209.

7 J. Yano and V. Yachandra, *Chem. Rev.* 2014**, 114**, 4175-4205.

8 B. M. Hoffman, D. Lukoyanov, Z.-Y. Yang, D. R. Dean and L. C. Seefeldt, *Chem. Rev.* 2014**, 114**, 4041-4062.

9 M. Can, F. A. Armstrong and S. W. Ragsdale, *Chem. Rev.* 2014**, 114**, 4149-4174.

10 A. I. Nguyen, M. S. Ziegler, P. Oña-Burgos, M. Sturzbecher-Hohne, W. Kim, D. E. Bellone and T. D. Tilley, *J. Am. Chem. Soc.* 2015**, 137**, 12865-12872.

View Article Online
DOI: 10.1039/C9DT02503K

11 A. I. Nguyen, D. L. M. Suess, L. E. Darago, P. H. Oyala, D. S. Levine, M. S. Ziegler, R. D. Britt and T. D. Tilley, *J. Am. Chem. Soc.* 2017**, 139**, 5579-5587.

12 A. I. Nguyen, L. E. Darago, D. Balcells and T. D. Tilley, *J. Am. Chem. Soc.* 2018**, 140**, 9030-9033.

13 A. W. Rutherford and A. Boussac, *Science* 2004**, 303**, 1782-1784.

14 Y. Umena, K. Kawakami, J.-R. Shen and N. Kamiya, *Nature* 2011**, 473**, 55-60.

15 I. D. Young, M. Ibrahim, R. Chatterjee, S. Gul, F. D. Fuller, S. Koroidov, A. S. Brewster, R. Tran, R. Alonso-Mori, T. Kroll, T. Michels-Clark, H. Laksmono, R. G. Sierra, C. A. Stan, R. Hussein, M. Zhang, L. Douthit, M. Kubin, C. de Lichtenberg, L. Vo Pham, H. Nilsson, M. H. Cheah, D. Shevela, C. Saracini, M. A. Bean, I. Seuffert, D. Sokaras, T.-C. Weng, E. Pastor, C. Weninger, T. Fransson, L. Lassalle, P. Bräuer, P. Aller, P. T. Docker, B. Andi, A. M. Orville, J. M. Glownia, S. Nelson, M. Sikorski, D. Zhu, M. S. Hunter, T. J. Lane, A. Aquila, J. E. Koglin, J. Robinson, M. Liang, S. Boutet, A. Y. Lyubimov, M. Uervirojnangkoorn, N. W. Moriarty, D. Liebschner, P. V. Afonine, D. G. Waterman, G. Evans, P. Wernet, H. Dobbek, W. I. Weis, A. T. Brunger, P. H. Zwart, P. D. Adams, A. Zouni, J. Messinger, U. Bergmann, N. K. Sauter, J. Kern, V. K. Yachandra and J. Yano, *Nature* 2016**, 540**, 453-457.

16 K. N. Ferreira, T. M. Iverson, K. Maghlaoui, J. Barber and S. Iwata, *Science* 2004**, 303**, 1831-1838.

17 J. H. Robblee, R. M. Cinco and V. K. Yachandra, *Biochim. Biophys. Acta (BBA) - Bioenergetics* 2001**, 1503**, 7-23.

18 C. Zhang, C. Chen, H. Dong, J.-R. Shen, H. Dau and J. Zhao, *Science* 2015**, 348**, 690-693.

19 J. S. Kanady, E. Y. Tsui, M. W. Day and T. Agapie, *Science* 2011**, 333**, 733-736.

20 S. Mukherjee, J. A. Stull, J. Yano, T. C. Stamatatos, K. Pringouri, T. A. Stich, K. A. Abboud, R. D. Britt, V. K. Yachandra and G. Christou, *Proc. Nat. Acad. Sci.* 2012**, 109**, 2257-2262.

21 H. Furutachi and H. Ōkawa, *Inorg. Chem.* 1997**, 36**, 3911-3918.

22 S. Kita, H. Furutachi and H. Ōkawa, *Inorg. Chem.* 1999**, 38**, 4038-4045.

23 S. K. Langley, N. F. Chilton, B. Moubaraki and K. S. Murray, *Dalton Trans.* 2012**, 41**, 1033-1046.

24 R. E. P. Winpenny, *J. Chem. Soc., Dalton Trans.* 2002**,** 1-10.

25 D. S. Nesterov, O. V. Nesterova, V. N. Kokozay and A. J. L. Pombeiro, *Eur. J. Inorg. Chem.* 2014**, 2014**, 4496-4517.

26 O. Stetsiuk, O. V. Nesterova, V. N. Kokozay, K. V. Domasevitch, I. V. Omelchenko, O. V. Shishkin, B. Vranovičová, R. Boča, A. J. L. Pombeiro and S. R. Petrusenko, *Dalton Trans.* 2017**, 46**, 7480-7494.

27 O. V. Nesterova, E. N. Chygorin, V. N. Kokozay, V. V. Bon, I. V. Omelchenko, O. V. Shishkin, J. Titiš, R. Boča, A. J. L. Pombeiro and A. Ozarowski, *Dalton Trans.* 2013**, 42**, 16909-16919.

28 D. S. Nesterov, E. N. Chygorin, V. N. Kokozay, V. V. Bon, R. Boča, Y. N. Kozlov, L. S. Shul'pina, J. Jezierska, A. Ozarowski, A. J. L. Pombeiro and G. B. Shul'pin, *Inorg. Chem.* 2012**, 51**, 9110-9122.

29 O. Stetsiuk, A. El-Ghayoury, V. N. Kokozay, N. Avarvari and S. R. Petrusenko, *J. Coord. Chem.* 2018**, 71**, 68-77.

30 D. S. Nesterov, V. N. Kokozay and B. W. Skelton, *Eur. J. Inorg. Chem.* 2009, 5469-5473.

31 D. S. Nesterov, V. N. Kokozay, B. W. Skelton, J. Jezierska and A. Ozarowski, *Dalton Trans.* 2007, 558-564.

32 G. Durgaprasad, D. N. Sathyanarayana and C. C. Patel, *Bull. Chem. Soc. Jpn.*, 1971, **44**, 316-322.

33 U. Bemm, R. Norrestam, M. Nygren and G. Westin, *Acta Crystallogr., Sect. C* 1995**, 51**, 1260-1263.

34 U. Bemm, K. Lashgari, R. Norrestam, M. Nygren and G. Westin, *J. Solid State Chem.* 1993**, 103**, 366-374.

35 S. Wörl, H. Pritzkow, I. O. Fritsky and R. Krämer, *Dalton Trans.* 2005**,** 27-29.

36 R. Modak, Y. Sikdar, A. Bieńko, M. Witwicki, M. Jerzykiewicz and S. Goswami, *Polyhedron* 2016**, 119**, 202-215.

37 I. D. Brown and D. Altermatt, *Acta Crystallogr., Sect. B* 1985**, 41**, 244-247.

38 R. M. Wood and G. J. Palenik, *Inorg. Chem.* 1998**, 37**, 4149-4151.

39 W. Liu and H. H. Thorp, *Inorg. Chem.* 1993**, 32**, 4102-4105.

40 P. V. Bernhardt and G. A. Lawrance, 6.1 - Cobalt. In *Comprehensive Coordination Chemistry II*, McCleverty, J. A.; Meyer, T. J., Eds. Pergamon: Oxford, 2003; pp 1-145.

41 J. F. Watts and J. Wolstenholme*, An introduction to surface analysis by XPS and AES*, Wiley, 2003, Chichester, ISBN 0-470 84713 1.

42 J.-G. Kim, D. L. Pugmire, D. Battaglia and M. A. Langell, *Appl. Surf. Sci.*, 2000, **165**, 70-84.

43 B. J. Tufts, Ian L. Abrahams, C. E. Caley, S. R. Lunt, G. M. Miskelly, M. J. Sailor, P. G. Santangelo, N. S. Lewis, A. Lawrence Roe and K. O. Hodgson, *J. Am. Chem. Soc.*, 1990, **112**, 5123-5136.

44 D. G. Brown and U. Weser, *Z. Naturforsch.*, 1979, **34B**, 1468-1470.

45 A.-J. Zhou, J.-L. Liu, R. Herchel, J.-D. Leng and M.-L. Tong, *Dalton Trans.* 2009**,** 3182-3192.

View Article Online
DOI: 10.1039/C9DT02503K

46 B. Fleury, L. Catala, V. Huc, C. David, W. Z. Zhong, P. Jegou, L. Baraton, S. Palacin, P.-A. Albouy and T. Mallah, *Chem. Commun.*, 2005, 2020-2022.

47 O. A. Adebayo, K. A. Abboud and G. Christou, *Inorg. Chem.* 2017**, 56**, 11352-11364.

48 A. Saha, M. Thompson, K. A. Abboud, W. Wernsdorfer and G. Christou, *Inorg. Chem.* 2011**, 50**, 10476-10485.

49 L. M. Wittick, L. F. Jones, P. Jensen, B. Moubaraki, L. Spiccia, K. J. Berry and K. S. Murray, *Dalton Trans.* 2006, 1534-1543.

50 A. Saha, K. A. Abboud and G. Christou, *Inorg. Chem.* 2011**, 50**, 12774-12784.

51 T. C. Stamatatos, K. M. Poole, K. A. Abboud, W. Wernsdorfer, T. A. O'Brien and G. Christou, *Inorg. Chem.* 2008**, 47**, 5006-5021.

52 E. N. Chygorin, O. V. Nesterova, J. A. Rusanova, V. N. Kokozay, V. V. Bon, R. Boča and A. Ozarowski, *Inorg. Chem.* 2012**, 51**, 386-396.

53 E. N. Chygorin, V. N. Kokozay, I. V. Omelchenko, O. V. Shishkin, J. Titiš, R. Boča and D. S. Nesterov, *Dalton Trans.* 2015**, 44**, 10918-10922.

54 T. Afrati, C. Dendrinou-Samara, C. P. Raptopoulou, A. Terzis, V. Tangoulis and D. P. Kessissoglou, *Angew. Chem. Int. Ed.* 2002**, 41**, 2148-2150.

55 C. J. Milios, S. Piligkos, A. R. Bell, R. H. Laye, S. J. Teat, R. Vicente, E. McInnes, A. Escuer, S. P. Perlepes and R. E. P. Winpenny, *Inorg. Chem. Commun.* 2006**, 9**, 638-641.

56 G. Karotsis, L. F. Jones, G. S. Papaefstathiou, A. Collins, S. Parsons, T. D. Nguyen, M. Evangelisti and E. K. Brechin, *Dalton Trans.* 2008**,** 4917-4925.

57 J. Cano *VPMAG*, University of Valencia, Spain: 2001.

58 R. Ruiz-García, E. Pardo, M. C. Muñoz and J. Cano, *Inorg. Chim. Acta* 2007**, 360**, 221-232.

59 M. J. T. Frisch, G. W.; Schlegel, H. B.; Scuseria, G. E.; Robb, M. A.; Cheeseman, J. R.; Scalmani, G.; Barone, V.; Mennucci, B.; Petersson, G. A.; Nakatsuji, H.; Caricato, M.; Li, X.; Hratchian, H. P.; Izmaylov, A. F.; Bloino, J.; Zheng, G.; Sonnenberg, J. L.; Hada, M.; Ehara, M.; Toyota, K.; Fukuda, R.; Hasegawa, J.; Ishida, M.; Nakajima, T.; Honda, Y.; Kitao, O.; Nakai, H.; Vreven, T.; Montgomery Jr.; J. A., Peralta, J. E.; Ogliaro, F.; Bearpark, M.; Heyd, J. J.; Brothers, E.; Kudin, K. N.; Staroverov, V. N.; Kobayashi, R.; Normand, J.; Raghavachari, K.; Rendell, A.; Burant, J. C.; Iyengar, S. S.; Tomasi, J.; Cossi, M.; Rega, N.; Millam, J. M.; Klene, M.; Knox, J. E.; Cross, J. B.; Bakken, V.; Adamo, C.; Jaramillo, J.; Gomperts, R.; Stratmann, R. E.; Yazyev, O.; Austin, A. J.; Cammi, R.; Pomelli, C.; Ochterski, J. W.; Martin, R. L.; Morokuma, K.; Zakrzewski, V. G.; Voth, G. A.; Salvador, P.; Dannenberg, J. J.; Dapprich, S.; Daniels, A. D.; Farkas, Ö.; Foresman, J. B.; Ortiz, J. V.; Cioslowski, J.; Fox, D. J., *Gaussian 09 (Revision A.2)*, Gaussian, Inc., Wallingford CT: 2009.

60 C. Lee, W. Yang and R. G. Parr, *Phys. Rev. B* 1988**, 37**, 785-789.

View Article Online
DOI: 10.1039/C9DT02503K

61 A. D. Becke, *J. Chem. Phys.* 1993, **98**, 5648-5652.

62 A. D. Becke, *Phys. Rev. A* 1988, **38**, 3098-3100.

63 A. Schäfer, H. Horn and R. Ahlrichs, *J. Chem. Phys.* 1992, **97**, 2571-2577.

64 A. Schäfer, C. Huber and R. Ahlrichs, *J. Chem. Phys.* 1994, **100**, 5829-5835.

65 E. Ruiz, A. Rodríguez-Fortea, J. Cano, S. Alvarez and P. Alemany, *J. Comput. Chem.* 2003, **24**, 982-989.

66 E. Ruiz, J. Cano, S. Alvarez and P. Alemany, *J. Comput. Chem.* 1999, **20**, 1391-1400.

67 E. Ruiz, J. Cano, S. Alvarez and P. Alemany, *J. Am. Chem. Soc.* 1998, **120**, 11122-11129.

68 J. Tomasi, B. Mennucci and E. Cancès, *J. Mol. Struct.: THEOCHEM* 1999, **464**, 211-226.

69 G.M. Sheldrick, SHELXL-97, Program for Crystal Structure Solution;University of Göttingen: Göttingen, Germany, 1997.

70 Rigaku Oxford Diffraction (2015). *CrysAlis PRO*. Rigaku Oxford Diffraction, Yarnton, England.

71 Diamond - Crystal and Molecular Structure Visualization, Crystal Impact - Dr. H. Putz & Dr. K. Brandenburg GbR, Kreuzherrenstr. 102, 53227 Bonn, Germany

Table of contents

View Article Online
DOI: 10.1039/C9DT02503K

Co-existence of ferro- and antiferromagnetic interactions in a hexanuclear mixed-valence $Co^{III}_2Mn^{II}_2Mn^{IV}_2$ cluster sustained by a multidentate Schiff base ligand:

An unprecedented hexanuclear mixed-valence $Co^{III}_2Mn^{II}_2Mn^{IV}_2$ cluster has been synthesized and structurally characterized. In depth magnetochemical investigations combined with DFT calculations demonstrate the co-existence of antiferro- and ferromagnetic interactions within the $Mn^{IV}_2Mn^{II}_2$ core.